International Journal of Microwave and Wireless Technologies, 2015, 7(3/4), 453–458.
doi:10.1017/S1759078715000550

RESEARCH PAPER

Coherent radiometric imaging using antennas with beam synthesizing

KONSTANTIN A. LUKIN, VOLODYMYR V. KUDRIASHOV, PAVLO L. VYPLAVIN, VOLODYMYR P. PALAMARCHUK AND SERGII K. LUKIN

The paper is devoted to coherent radiometric imaging systems. The investigated systems may be considered as a version of bistatic noise waveform passive radar with synthetic aperture having external reference. Reference signal in this imaging system is received from the investigated emitting object using auxiliary receiver. Although a number of theoretical studies on aperture synthesis imaging algorithms exist, relatively few of them deal with experimental investigation. In particular, no information concerning range-azimuth coherent radiometric imaging has been found. In this paper, an experimental investigation of possibility to generate coherent radiometric images using two antennas with beam synthesizing is carried out. Indoor radiometric imaging has been validated using absorbers as the emitting objects. These experiments enabled to estimate range resolution of the radiometric system achieved by focusing antennas with beam synthesizing for range span limited by means about bistatic baseline.

Keywords: Microwave measurements, Radar applications

Received 11 November 2014; Revised 27 February 2015; Accepted 5 March 2015; first published online 4 June 2015

I. INTRODUCTION

Radiometric monitoring allows obtaining information about thermal electromagnetic radiation of emitting objects in the chosen frequency band. Imaging of distant emitting objects using their thermal electromagnetic radiation may be implemented with the help of bistatic radiometric systems [1–3]. This approach has been developed in long wave radar astronomy to improve angular resolution of telescopes [4, 5].

Imaging in millimeter waveband is often done using multichannel reception via antenna array and mechanical or frequency scanning along the axis perpendicular to the array plane [6]. Further development of this approach consists of realization of two-dimensional (2D) aperture synthesis which enables radiometric coherent imaging in the plane perpendicular to the antenna beam. Such images contain not only amplitude information but also information concerning relative phase [7].

We consider the generation of radiometric images in the range-azimuth plane. Spatial diversity of two antennas enables estimation time difference of arrival (TDOA) of incoming signals. The TDOA estimate may be done via the cross-correlation technique. It is based upon cross-correlation of signals coming to two receivers. The TDOA estimation is provided as the location of the peak of the cross-correlation estimate. This requires an auxiliary channel (receiver and antenna). The receivers' bandwidth limits the angular resolution of such setup.

There is a possibility of coherent radiometric imaging using combination of information on the bistatic radiometer (BR) response and angular position of narrow beam of antenna with beam synthesizing (ABS) at one (or both) of the receivers. Each pixel of such image can be obtained as focusing of equal TDOA area via the pattern of the ABS. Besides, the factors limiting usage of this approach and possibility of obtaining of 2D resolution using combination of BR data and principles of aperture synthesis have not been investigated yet. This paper is devoted to investigation of coherent radiometric imaging in range-azimuth plane via proving the concept of 2D imaging by BR with two ABS. Experimental investigations have been carried out using ground-based Ka-band BR with ABS based upon Ka-Band Bistatic Ground-Based Noise Waveform SAR equipment [8, 9].

II. COHERENT RADIOMETRIC IMAGING

The proposed approach to coherent radiometric imaging consists of using BR and moving of the antennas for realizing synthetic apertures. This scheme enables obtaining range resolution of emitting objects at distances comparable with bistatic baseline. This is possible due to the fact that shifting of one antenna of interferometric radiometer with respect to stable emitting object changes phase relations between received signals. For different positions of the emitting object these phase relations will depend on antenna positions

Laboratory for Nonlinear Dynamics of Electronic Systems (LNDES), O.Ya. Usikov Institute for Radiophysics and Electronics, National Academy of Sciences of Ukraine, 12 Ak. Proskura Str., Kharkiv 61085, Ukraine. Phone: +38050 3232756
Corresponding author:
K. A. Lukin
Email: lukin.konstantin@gmail.com

in different way. This fact can be used for building a reference function (a function of antenna position) and performing co-variation of radiometer returns with it. This gives a chance to improve the resolution and to some limit to generate 2D images. The paper is devoted to investigation of possibility and constraints of generation of 2D images using this approach at short ranges.

For realization of spatial scanning we use ABS [1, 2]. Phase centers of antennas are moved along a real aperture in stepped like manner and signals are being recorded only when the antennas are stationary. This enables using common in SAR principle of splitting of the processing into two parts. The first step of coherent radiometric imaging is to perform cross-correlation between signals received in two channels. This will give information concerning mutual path length difference between signals. The second stage consists of co-variation of those signals obtained in different positions of ABS with corresponding reference function.

TDOA of the signal $\Delta\tau(x, y)$ coming to receiver and to the auxiliary receiver equals to $\Delta l\,(x,\ y)/c$, where $\Delta l\,(x,\ y) = l_1\,(x,\ y) - l_2\,(x,\ y)$ is path length difference between the emitting object with range-cross range coordinates (x, y) to the receiving antennas [3]. Mutual path length difference $\Delta l(x, y)$ cannot exceed the bistatic baseline l_B. At each of antenna positions a the value of TDOA equals:

$$\Delta\tau_a(x,\ y) = \Delta l_a\,(x,\ y)/c. \tag{1}$$

Cross-correlation function between signals received by reference channel of imager $S_{1,a}(t+\tau)$ and the auxiliary receiver $S^*_{2,a}(t+\tau_a)$ can be estimated as:

$$R_a(\tau,\ T) = \frac{1}{T}\int_0^T S_{1,a}(t+\tau)S^*_{2,a}(t+\tau_a)d\tau, \tag{2}$$

where T is the integration time; $\tau \in [-l_B/c;\ l_B/c]$ is the mutual delay of the signals introduced for compensation of (1); symbol * denotes complex conjunction. The delay τ introduced in (2) may compensate TDOA value τ_a which may exceed the incoming signal coherence time. Thus the bistatic baseline is not limited by the coherence length of the signal.

Compression of the signals by path length difference consists of estimation of cross-correlation $R_a(\tau,\ T)$ for the required TDOA values and for all antenna positions.

Movement of phase center of ABS [1, 2] causes change in path of the radio waves in waveguide. This change has to be taken into account during signal processing. Estimation of phase shift is easier to perform in frequency domain by adding corresponding phase shifts to all of the frequency components of the signals. Using known [10] relation for the main wave of rectangular waveguide this phase shift can be estimated using the following relation:

$$\phi_a(\lambda_i) = 2\pi\, l_a \sqrt{\frac{\xi\,\mu}{\lambda_i^2} - \frac{1}{(2p)^2}}, \tag{3}$$

where $\lambda_i = c/f_i$ is the wavelength of the given frequency f_i in free space; l_a is waveguide length corresponding to antenna position a; ξ, μ are the relative electric and magnet permittivity; p is the width of wide wall of the waveguide.

For effectiveness, correlation processing (2) has been performed in frequency domain using a fast Fourier transform. Taking into account (3) the cross-correlation (2) of the received signals is:

$$R_a(\tau) = \langle S^*_{1,\,a}(\omega_i)\; S_{2,\,a}(\omega_i)\;\exp\big(j\phi_a(\omega_i) + j\omega_i\tau\big)\rangle, \tag{4}$$

where $\omega_i = 2\pi f_i$ is the circular frequency of the received waveform spectrum limited by the BR band pass $\omega_i \in [\omega_{\min};\ \omega_{\max}]$; symbols $\langle\rangle$ denote statistical averaging over ω_i.

The second step of the processing uses the results of correlation processing (3). It consists of estimation of the base of theoretical response from current point of space an expected variation of radar returns as a function of antenna position. Then, the received signals are compared with this reference function via co-variation. Relation for the generation of coherent radiometric image $I(x,\ y)$ in time domain and with common simplification consisting of neglecting of amplitude term of reference function has the following form:

$$I(x,\ y) = \langle R_a\big[\Delta\tau_a(x,\ y)\big]\rangle\;\exp\big[-j\omega_c\,\Delta\tau_a(x,\ y)\big], \tag{5}$$

where ω_c is the circular carrier frequency of the received waveform spectrum; and symbols $\langle\rangle$ denote averaging over antenna positions in the performed scan.

Thus, coherent radiometric image generation (5) consists of (a) matched filtration of the received signals and (b) the signals averaging up with taking into account phase difference between emitting object signals received by the BR antennas.

III. KA-BAND BR WITH ANTENNAS WITH BEAM SYNTHESIZING

The current work is devoted to the experimental evaluation of the possibility to obtain range resolution on coherent radiometric images with the Ka-Band Bistatic Ground-Based Noise Waveform SAR equipment modified for operation in the radiometric mode. The Ka-band BR (Fig. 1) uses the new type of antennas – ABS [1, 2].

A) Antennas with beam synthesizing

This is a special type of antennas phase center of which is moved along a real aperture (Fig. 2). As a real aperture

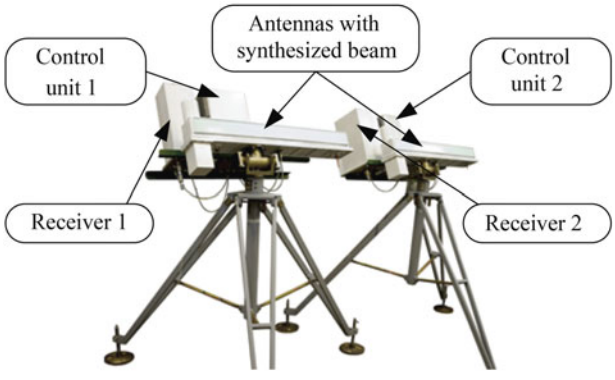

Fig. 1. Picture of the Ka-band BR with antennas with beam synthesizing.

https://doi.org/10.1017/S1759078715000550 Published online by Cambridge University Press

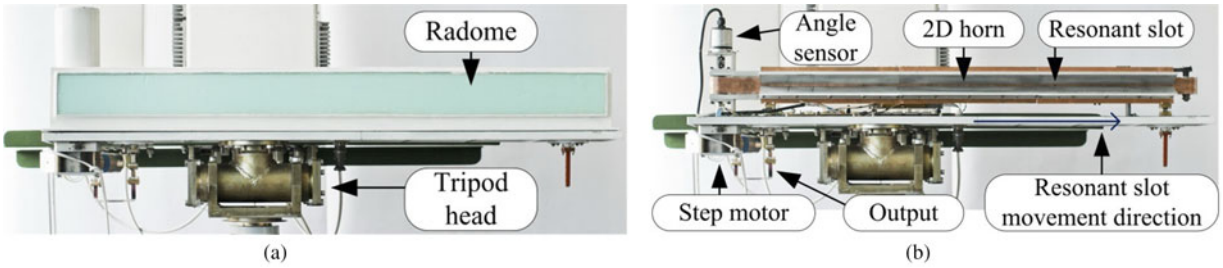

Fig. 2. Ka-band ABS: (a) general view of the reception point; (b) sub-units of the antenna.

antenna, a waveguide with a non-radiating half-wavelength longitudinal slot in its wider wall is used. The wall is covered with a metallic tape having a half-wavelength transverse resonant slot. In order to enhance its efficiency we placed a sliding plunger tied to the tape at the proper distance from the radiating slot. The tape moves along precise guides. Position of the slot is controlled by angle sensor. In the work, phase centers of antennas are moved in stepped like manner and signals are processed only when the antennas are stationary.

B) The BR processing gain test

The Ka-band BR with ABS enable the generation of coherent radiometric images in 36.0–36.5 GHz band. The estimated bandwidth of receivers equals to 465 MHz. The noise factor of each receiver is 3 (noise temperature is 600 K). Estimated gain of receivers is up to 97 dB. Each receiver output signal is fed to 8-bit ADC with bandwidth 500 MHz (GaGe CS22G8-1 GHz) and saved to HDD for post-processing.

Received signals of thermal radiation of emitting objects are quite weak that leads to necessity of increasing the processing gain. The leakage of signals between two receivers (represents interchannel interference) limits opportunity of signal-to-noise ratio (SNR) improvement via processing gain increasing. We have carried out estimation of the leakage in Ka-band BR with ABS. Namely we have investigated dependence of output SNR on integration time in the limits of the processing gain of 20–70 dB. This has been done using two schemes shown in Fig. 3. The first scheme enabled to evaluate processing gain for the case of two correlated signals input to the digital correlator. Output SNR is close to input SNR multiplied by the processing gain. The second one consisted of feeding two uncorrelated signals to the correlator. It was done in order to estimate the correlator output signal power decrease along the integration time increasing. The output SNR showed good agreement with the expected processing gain. It proved that the leakage of the Ka-band BR with ABS is low enough for our radiometric experiments. This isolation level is provided by the down converter scheme where the oscillations frequency of common X-band oscillator is

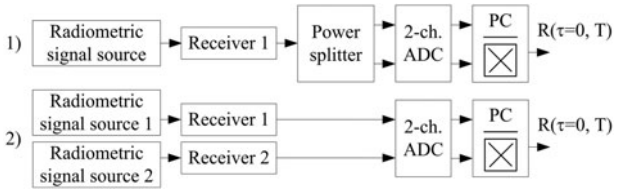

Fig. 3. Block-schemes for the estimation of the leakage of signals between two receivers.

multiplied by 4 separately for each channel [8, 11]. The receivers' synchronization is provided by: (a) the down converter oscillator that is common in two receivers and (b) the ADC clock generator that is common in two receivers. The oscillator signal is transferred to the auxiliary receiver via coaxial cable. The baseline extension can affect the transferred signal performance that will decrease the system performance.

IV. EXPERIMENTAL SETUP

The aim of the experiment was to generate coherent radiometric images using Ka-band BR with ABS.

A) The BR performance estimation

In order to validate ability of the radiometer to detect emitting objects on the background of the intrinsic noise of the receivers and to detect difference in thermal radiation of emitting objects it is necessary to measure the minimal increase of the signal amplitude which can be registered by the equipment. To check operation of the equipment in radiometric regime we used two stable dish antennas with 0.34 m diameter and regime of interferometric radiometer without spatial scanning with ABS [1, 2]. To compare the output levels with the noise floor we used to switch matched loads to the inputs of the receivers between measurements with dish antennas. The experiment cycle was as following: (a) matched loads are connected to the receivers' inputs, (b) two Ka-band dish antennas are connected to the inputs and directed to the sky, (c) matched loads are connected to the receivers' inputs, and (d) the antennas are connected to the receivers' inputs and directed to the concrete room ceiling. The integration time of 4 s was used in the cycle. In order to compare different realizations of these responses the cycle was repeated three times. That is why the Fig. 4 shows three realizations for the radiometer responses on sample emitting objects as the sky and the ceiling and 6 realization for the noise floor. Temporal intervals for re-connection of antennas and their direction affected total measurement time about few hours. The output levels of the radiometer (Fig. 4(b)) show that the difference in intrinsic noise level, the sky and the ceiling can be recognized, but changing in time the radiometer equipment parameters lead to some variations in the output levels for each of the emitting objects.

B) Coherent radiometric imaging experiment

For the coherent radiometric imaging experiment the equipment was placed inside a laboratory room. The phase delay of signal passes along antennas and receivers has been taken

https://doi.org/10.1017/S1759078715000550 Published online by Cambridge University Press

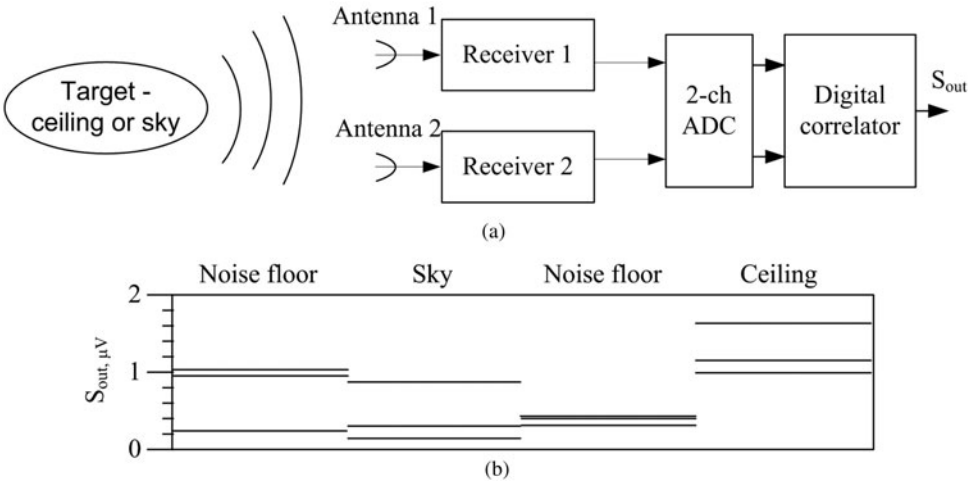

Fig. 4. The radiometer output signal level: intrinsic noise, sky, and room ceiling: (a) the experiment scheme; (b) the radiometer output signal levels, three experiment cycles results.

into account by calibration measurements using noise waveform generator placed. Ka-band noise waveform generators were used for the indoor preliminary experiments. They showed good concordance between the generators positions and coordinates of the generated radiometric images' peaks. The experiments showed intersection of sidelobes of the Ka-band BR with ABS.

For proof of concept of indoor coherent radiometric imaging two absorbers were placed behind a window (Fig. 5). The room inside temperature was about 293 K.

Correlation processing of received signals has been performed in frequency domain. The sidelobe level can be improved by applying weighting function to spectrums of

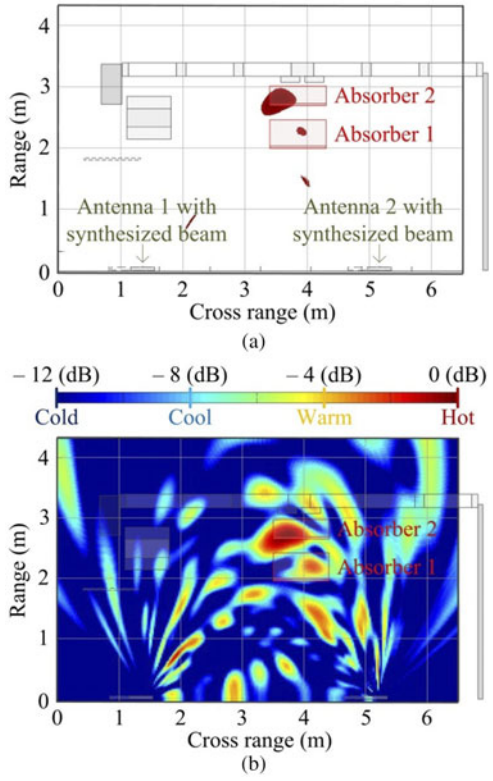

Fig. 5. Generated images of the room interior for different threshold levels: (a) threshold equals to −3 dB; (b) threshold equals to −12 dB.

received. Coherent radiometric imaging has been done taking into account the TDOA of the emitted signals to each receiver antenna (5). Step-like moving of phase centers of the ABS and the approach to generation of coherent radiometric images enabled to generate coherent radiometric image. The image contains amplitude and phase information along coordinates (range and cross-range directions). Logarithmic values of amplitude in each pixel are shown (Fig. 5). This amplitude information corresponds to apparent temperature of the objects in the scene. Semitransparent scheme of objects location inside is shown in the figure as well. The −3 dB threshold was applied to the color scheme (Fig. 5(a)) in order to analyze the image. Two peaks coincide the absorbers positions. The peaks positions are shifted from the absorbers centers. Another two peaks (in range span up to 2 m) do not coincide the absorbers positions.

The numerical simulation was provided to check the essence of the shifts. The simulation included the experiment geometry and the Ka-band BR with ABS parameters. It showed that the shift may be explained by close separation between the absorbers. The responses interaction does not lead to shift of their maxima at larger distances. The simulation showed the sidelobes interaction mentioned above as well. The interactions may cause false peaks on images. The peaks in range span up to 2 m may be explained by combination of sidelobes of two targets. Threshold by −12 dB was applied to color scheme (Fig. 5(b)). The scheme shows low amplitude (low apparent temperatures) with tints of blue color and high amplitude with tints of reds.

The strongest response in the image (Fig. 5(b)) corresponds to the object with rough surface (absorber 2). Absorber range is 2.6 m and cross-range is 3.7 m. The weaker responses in the image correspond to false peaks as well as to objects with smooth surfaces (the painted concrete wall, the window, the linoleum-covered floor). The response from object with smooth surface (related to the range 2.7 m and cross-range 3 m) is lower than the response from the object with rough surface by 19.7 dB. The object with rough surface emissivity ε_R equals to 0.98 and the object with smooth surface emissivity ε_S equals to 0.95 when zenith angle is 20° [3]. This provides an expected brightness temperature contrast of $\Delta T = T(\varepsilon_R - \varepsilon_S) \approx 9$ K. With respect to the radiation efficiency of the antenna and scene

https://doi.org/10.1017/S1759078715000550 Published online by Cambridge University Press

temperature measured by the antenna pattern sidelobes, the minimum detectable temperature change on the image equals to $9/10^{1.97} \approx 0.1$ K. The calculated sensitivity value matches the experimentally obtained value well enough. Generally, cleaner images may be obtained in the case of increasing of SNR of the radiometric system.

The possibility of coherent radiometric images generation using Ka-band BR with ABS is shown. Its range resolution depends on the antennas apertures length and position of emitting object.

C) Data transfer in the Ka-band BR with ABS

The synthetic aperture was formed by 51 antenna positions from each of the channels. At each position of phase centers of ABS 10^9 samples of data have been acquired at 1 giga-samples per second. These samples were transferred from random-access memory to hard disc drive of personal computer as data packets of 256 mega-samples. Thus total integration time was 51 s. It was performed an integration of estimated cross-correlation functions (equation 4) in frequency domain. Particularly, estimated cross-correlation functions of such data packets were averaged. It was done with respect to their phase structure.

V. ESTIMATION OF RESOLUTION CELL DIMENSIONS OF GENERATED IMAGES

Angular resolution of interferometric radiometer is well known. Angular resolution provided by the ABS is also known from theory of SAR. The current work investigates unusual combination of these techniques which provides the range and azimuth measurement. This section is devoted to estimation of the resolution in both coordinates. Estimation of the position of emitting object in the range-azimuth plane requires data on the emitter of thermal radiation azimuth β and path length difference R. The provided coherent radiometric imaging focuses the target positions on the equal TDOA area by the ABS. The response of the coherent radiometric imager may be considered as intersection of the synthesized beam maxima with maxima of path length difference hyperbolic response R. The point of the maxima intersection is denoted as T (Fig. 6). Distance (slant range) r to point T can be defined using law of cosines as follows:

$$r_1^2 = r^2 + B^2 - 2rb\ \cos(\beta), \tag{6}$$

where $r_1 = r - R$; b the baseline of the BR. Then reduction of similar terms of this expression enables to express r as follows:

$$r = \frac{R^2 - B^2}{2\left[R - B\ \cos(\beta)\right]}. \tag{7}$$

Thus, the range to the emitter is calculated based on the distance between the phase centers of the receiving antennas b, the result of estimation of the path length difference R and the result of estimation of the azimuth β.

Let us denote dimensions of resolution cell according to the position of the emitting object. These dimensions are limited by both width of the hyperbola (between DA and CB, Fig. 6) and by the width of the synthesized beam (between OA OD,

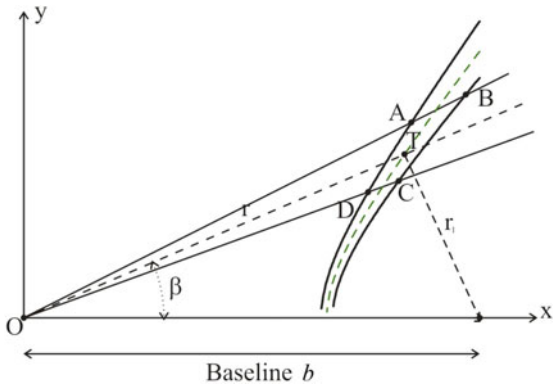

Fig. 6. Explanation to the estimation of coordinates in the range-azimuth plane.

Fig. 6). Azimuth increasing affects the range size of the curvilinear quadrangle *ABCD*.

Dimensions of the curvilinear quadrangle *ABCD* (Fig. 6) can be estimated by means of its projections on the axes of coordinates. Equation (7) is suitable for calculations of distances to its vertices *A*, *B*, *C*, and *D*. The measured values of azimuth allow calculating projections of segments *OA*, *OB*, *OC*, and *OD* to the specified axis. This calculation approach takes into account data on carrier wavelength and wave propagation velocity, azimuth and corresponding size of synthesized apertures, bandwidth of received signals, paths difference of arrival and bistatic baseline. The desired dimensions of the curvilinear quadrangle *ABCD* are defined as distances between the maximum and minimum coordinates of its vertices.

Numerical simulation of the dimensions of the curvilinear quadrangle *ABCD* had been provided. The simulation was provided using parameters of existing equipment. It was shown that its range size varies on propagation paths difference, bandwidth, antenna aperture, baseline, and others. For the system with one ABS, the curvilinear quadrangle *ABCD* range size got better with widening of the bandwidth, with shortening the range and for some azimuth values. The latest depends on the position of the ABS. Enlarging the baseline improves the range size of the quadrangle as well. For such geometry of the system, the range size of curvilinear quadrangle *ABCD* does not exceeds 0.6 m threshold only for some path lengths difference values and azimuth values from 10° to 40° approximately. Defining the limitation of such resolution cell (curvilinear quadrangle *ABCD*) as well as system parameters is suitable in order to estimate some limitations of a field of view.

It should be mentioned that the accuracies of estimation of both azimuth and path lengths difference are limited by existing SNR as well as by losses in the BR equipment. That is why both resolution cell position and dimensions can be not equal to described ones.

VI. CONCLUSION

Approach for coherent radiometric imaging using BR with antennas with beam synthesizing has been proposed. Unlike other radiometric imaging methods, this approach enables the realization of the range resolution in radiometric measurements within the distances range that is comparable with the BR baseline. This approach has been tested using Ka-Band Bistatic Ground-Based Noise Waveform SAR equipment [8] modified

https://doi.org/10.1017/S1759078715000550 Published online by Cambridge University Press

for operation in the radiometric regime. It has been shown that the system can have processing gain of up to 70 dB without saturation by ADC dynamic range and cross channel isolation. Possibility to recognize emitting objects on the background of noise floor has been shown. The proposed approach has been tested experimentally. Coherent radiometric images of thermal noise signals emitting objects have been generated in the regime of BR with antennas with beam synthesizing. An approach to estimation of dimensions of resolution cell of the investigated system has been proposed. Operation in such regime has shown good agreement with theoretical expectations.

ACKNOWLEDGEMENT

The research work on the data processing, radiometric resolution capability estimations, and preparation of this paper for publication have been supported by FP-7 Project SCOUT, grant no. 607019, and by the Project AComIn "Advanced Computing for Innovation", grant no. 316087, funded by the FP7 Capacity Program (Research Potential of Convergence Regions).

REFERENCES

[1] Lukin, K.A.: Sliding antennas for noise waveform SAR. Appl. Radio Electron., **4** (2005), 103–106.

[2] Lukin, K.A.: Scanning synthetic radiation pattern antennas. Radioelectron. Commun. Syst., **53** (2010), 219–224.

[3] Dulevich, V.E. ed.: Theoretical Backgrounds of Radiolocation, Sov. Radio, Moscow, 1978. (In Russian).

[4] Edelsohn, C.R.; Wiley, C.A.: Interferometric radiometer, US patent, 1991, Feb. 5. 4990925.

[5] Thompson, A.R.; Moran, J.M.; Swenson, G.W. Jr: Interferometry and Synthesis in Radio Astronomy, 2nd ed., Wiley, New York, 2001.

[6] Shilo, S.A.; Komyak, V.A.: Millimeter band scanning multi-beam radiometer, in Proc. MSMW, Kharkov, Ukraine, 1998.

[7] Dong, J.; Shi, R.; Chen, K.; Li, Q.; Lei, W.: An external calibration method for compensating for the mutual coupling effect in large aperture synthesis radiometers. Int. J. Antennas Propag., **1** (2011), 1–8.

[8] Lukin, K.A. et al.: Ka-Band bistatic ground-based noise waveform SAR for short-range applications. IET Radar Sonar Nav., **2** (2008), 233–243.

[9] Tarchi, D.; Lukin, K.; Fortuny-Guach, J.; Mogyla, A.; Vyplavin, P.; Sieber, A.: SAR imaging with noise radar. IEEE Trans. Aerospace Electron. Syst., **46** (2010), 1214–1225.

[10] Nikolskiy, V.V.; Nikolskaya, T.I.: Electrodynamics and Propagation, Science, Moscow, 1989. (In Russian).

[11] Lukin, K.A.: Noise radar technology. J. Telecommun. Radio Eng., **55** (2001), 8–16. [Radiophysics and electronics, 4(1999), 105–111].

Konstantin A. Lukin received his diploma in Radiophysics and Electronics from Kharkov State University (KhSU), Ukraine, in 1973. Since 1973 he has been with the Institute for Radiophysics and Electronics, National Academy of Sciences of Ukraine, IRE NASU, Kharkov. He defended his Candidate of Science Thesis in Moscow State University (MGU) in 1980 and his Doctor of Sciences thesis he defended in KhSU in 1989. He has been working and made appreciable contributions in the fields of millimeter wave vacuum electronics, random signal processing, dynamical chaos, and Noise Radar Technology (NRT). His research interests are as follows: nonlinear dynamics and chaos in electronic systems; generation and processing of chaotic/noise waveforms and their applications. His main current activities lay in the field of NRT and its applications. He is a Fellow of IEEE.

Volodymyr V. Kudriashov, Ph.D., M.Sc., a research fellow of Laboratory for Nonlinear Dynamics of Electronic Systems of O.Ya. Usikov Institute for Radiophysics and Electronics of National Academy of Sciences of Ukraine, Kharkiv, Ukraine. The field of scientific interests: bistatic radiometers, signal processing, SAR imaging.

Pavlo L. Vyplavin, Ph.D. In 2004, he graduated from Kharkiv National University with M.S. degree in Radiophysics and Electronics. Since 2004 he has been with Laboratory of Nonlinear Dynamics of Electronic Systems of Usikov Institute for Radiophysics and Electronics of NAS of Ukraine. In 2005, he took part in in-service training at Joint Research Centre of the European Commission, Ispra, Italy where he studied SAR imaging using noise radars. His research interests are: noise radar technology, chaotic waveform generation and processing, SAR imaging, antenna arrays, and pulsed Doppler radar.

Volodymyr P. Palamarchuk, a leading engineer of the Laboratory for Nonlinear Dynamics of Electronic Systems of O.Ya. Usikov Institute for Radiophysics and Electronics of National Academy of Sciences of Ukraine, Kharkiv, Ukraine. The field of scientific interests: radar microwave technology.

Sergii K. Lukin was born in 1987. He graduated from Kharkiv National Aerospace University 2010 and joined Laboratory for Nonlinear Dynamics of Electronic Systems of O.Ya. Usikov Institute for Radiophysics and Electronics of National Academy of Sciences of Ukraine, Kharkiv, Ukraine. He currently holds the position of junior researcher. The field of interest: FPGA, signal processing, software-defined radar, and software development.

https://doi.org/10.1017/S1759078715000550 Published online by Cambridge University Press